Assessment of the hydrodynamic loads due to a LOCA in a 3-loop PWR. Castem-Plexus computations

Marie-France Robbe, Michel Lepareux, Christophe Trollat

▶ **To cite this version:**

Marie-France Robbe, Michel Lepareux, Christophe Trollat. Assessment of the hydrodynamic loads due to a LOCA in a 3-loop PWR. Castem-Plexus computations. ICONE8 - 8th International Conference on Nuclear Engineering, ASME, Apr 2000, Baltimore, United States. pp.ICONE-8199. cea-04044567

HAL Id: cea-04044567

https://cea.hal.science/cea-04044567

Submitted on 24 Mar 2023

HAL is a multi-disciplinary open access archive for the deposit and dissemination of scientific research documents, whether they are published or not. The documents may come from teaching and research institutions in France or abroad, or from public or private research centers.

L'archive ouverte pluridisciplinaire **HAL**, est destinée au dépôt et à la diffusion de documents scientifiques de niveau recherche, publiés ou non, émanant des établissements d'enseignement et de recherche français ou étrangers, des laboratoires publics ou privés.

Proceedings of ICONE8
8th International Conference on Nuclear Engineering
April 2-6, 2000, Baltimore, MD USA

ICONE-8199

ASSESSMENT OF THE HYDRODYNAMIC LOADS DUE TO A LOCA IN A 3-LOOP PWR. CASTEM-PLEXUS COMPUTATIONS

Marie-France ROBBE
CEA Saclay - DRN/DMT/SEMT - 91191 Gif sur Yvette cedex - FRANCE
Tel: (33.1) 69.08.87.49, Fax: (33.1) 69.08.52.42
E-mail: mfrobbe@cea.fr

Michel LEPAREUX *
CEA Saclay - DRN/DMT/SEMT/DYN - 91191 Gif sur Yvette cedex - FRANCE
Tel: (33.1) 69.08.40.18, Fax: (33.1) 69.08.83.31
E-mail: mlepareux@cea.fr

Christophe TROLLAT
EDF - SEPTEN - 12-14, av. Dutrievoz - 69628 Villeurbanne cedex - FRANCE

Keywords

blowdown, depressurization, LOCA, pipe, dynamic, hydrodynamic loads, primary circuit, PWR

Abstract

The safety analysis of the PWR plants requires to assess the consequences of a hypothetical Loss Of Coolant Accident in the whole primary circuit and the reactor. This paper is dedicated to the study of the depressurization phase immediately following the break opening and to the evaluation of the mechanical consequences of the transient on the inner structures of a 3-loop PWR.

The primary circuit and the reactor are represented with a pipe-model. A guillotine rupture is applied to one of the cold legs, just downstream the pump. The geometric model and the hydraulic conditions were described in (Robbe[a], 1999). This paper only deals with the analysis of the results calculated with the CASTEM-PLEXUS code.

We suppose that the LOCA occurs in a reactor working at nominal rating. A first calculation is carried out at nominal rating for 2 s in order to validate the numerical model. The validation is obtained by comparing the computed pressures, volumic flows and pump working conditions with the estimated nominal rating ones. As the computation converges around the initial data (approximating the nominal rating), then the model is correct and can be used for the LOCA computation.

A second calculation is performed during 500 ms, in accidental operation, from the previous initial conditions. The results are globally and locally scrutinized thanks to whole circuit drawings at a given time and local curves showing the evolution of a variable versus time. The analysis concerns the pressures and the volumic flows.

1 Introduction

The safety analysis of the PWR plants (Libmann, 1996) requires to assess the consequences of a hypothetical Loss Of Coolant Accident (LOCA).

The present research in mechanics is globally aimed at accident prevention (Van Goethem, 1999), vibrations (Payan, 1998) (Seligmannn 1997) able to initiate a break tearing, detection of potential cracks during in-service inspections (Riffard, 1999), crack opening and leak-before-break (Keim, 1999).

Copyright © 2000 by ASME

The thermalhydraulics studies are oriented towards the emptying of the primary circuit (Weiss, 1986) (Ludmann,1999), scenarios possibly leading to a core dryout (Pretel, 1998), the design of passive systems complementary to the Coolant Injection System in order to limit the reactor draining (Sardain, 1998), the thermal effects of the successive feed-and-bleeds on the core fuel assemblies (Ohvo, 1998), the coupling with neutronics (Royer, 1998)...

The present paper is devoted to an intermediary approach between mechanics and thermalhydraulics. It tries to assess the mechanical consequences of the blowdown phase on the reactor core by working out coupled acoustic and thermalhydraulic computations.

The CASTEM-PLEXUS code (Hoffmann, 1984) (Robbe[b], 1999) was chosen because it can deal with fluid-structure interaction and both pipe elements (Lepareux[a], 1985) (Lepareux[b], 1985) and 3D elements are available to model easily the primary circuit. This paper presents the first results obtained with a simplified model, only composed of rigid pipes.

The primary circuit (pipes and components) and the reactor are represented with a pipe-model (Fig. 1) respecting the 3D component capacities and the average distances covered by the water. These two criteria are useful to abide by the flow rate and the propagation time of the acoustic waves through the circuit. For the components, the pipe length is evaluated using the average water route inside each component zone.

The flow restrictions due to grids or perforated plates are not meshed but their hydraulic effects are taken into account thanks to pressure losses. The hydraulic model also takes into account the pump characteristic and the pressure losses by friction.

The water is described by a classical diphasic constitutive law (Papon, 1990) assuming that liquid water and steam are at equilibrium during the vaporization phase. The water thermodynamic parameters are given by steam tables (Haar, 1984).

A guillotine rupture is applied to the cold leg of the first loop, just downstream the pump. The break model is homogeneous (no phase slide) and respects the Moody hypothesises (Moody, 1965).

The calculations are initialized at the reactor nominal rating. A first calculation is carried out in normal operation in order to validate the numerical model. A second calculation is performed in accidental operation from the previous initial conditions. The results of both computations are described and analysed.

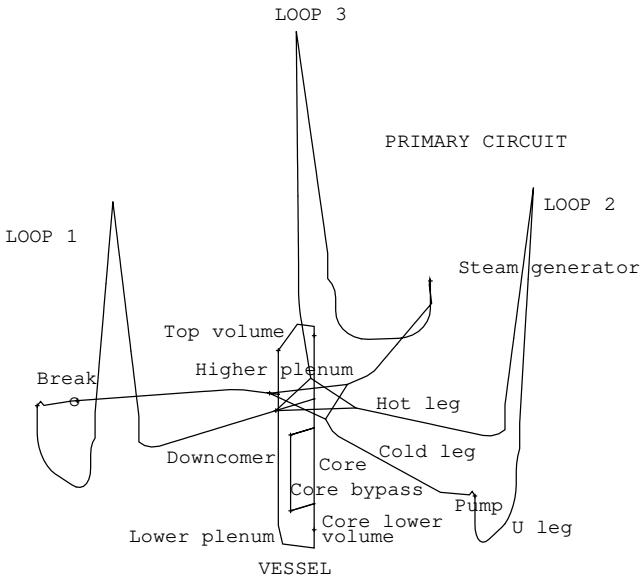

Figure 1: Pipe-model of a 3-loop PWR

2 Computation of the reactor nominal rating

As the computations of a LOCA in a real reactor are blind assessments with no possibility to compare the computed results with theoretical or experimental ones, the detection of a mistake in the numerical model is impossible. Thus a preliminary work of validation of the model is compulsory.

This validation is obtained by performing a computation at the normal operating conditions. The break is replaced by a connection between both pipe ends. As the computations are initialized approximately at the normal operating conditions, the convergence of the results around the initial conditions is sufficient to prove the model correctness.

Copyright © 2000 by ASME

The computation of the nominal rating is carried out for 2 s. From the geometrical data, the pressure drop coefficients, the pump characteristics and the approximated initial data, CASTEM-PLEXUS computes the local pressures, densities, velocities... along the circuit. Our aim is to check in the model consistency, and specially the volumic flow rates, the pressure losses, the density and the pump behaviour.

The figure 2 shows the volumic flow rates at a different place for each one of the three loops (steam generator of loop 1, pump of loop 2 and cold leg of loop 3) and at three places of the reactor (downcomer, core and reactor outlet).

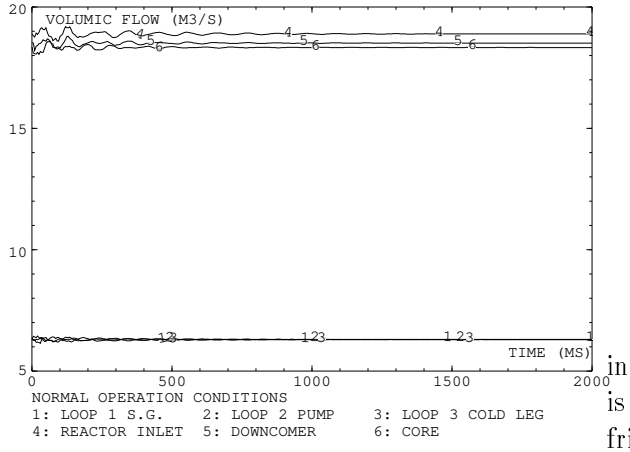

Figure 2: Flow rate

After some oscillations of small amplitude which damp very fast, the flow rates are perfectly stabilized around the initial values. The computed flow rates after 2 s fit in with the reactor nominal rating ones (Table 1).

	Nominal rating flow rates (m^3/s)	Computed flow rates (m^3/s)
Loops	6.3	6.3
Reactor inlet	18.9	18.9
Downcomer (98% of the total flow)	18.52	18.5
Core (99% of the main flow)	18.33	18.3

Table 1: Comparison of the theoretical and computed flow rates in the circuit

The figure 3 shows the pressure at several locations of the loops and the reactor. As the circuit is initialized at 15.5 MPa everywhere, the taking into consideration of the pressure losses and the pump thrust causes a large pressure variation at the beginning. The pressure balance in the circuit is obtained after nearly 1 s.

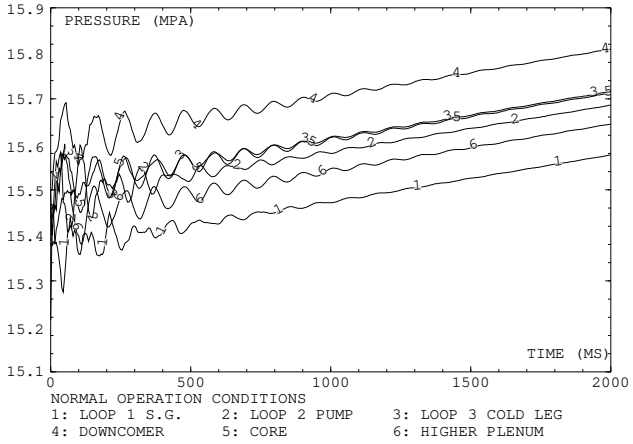

Figure 3: Pressure

The curves present a slight pressure increase in the process of time. Because the system is considered adiabatic, the pressure losses by friction induce a slight rise of the water temperature. As all the thermodynamic parameters are correlated in the water table, a temperature increment is immediately transformed into a pressure increment.

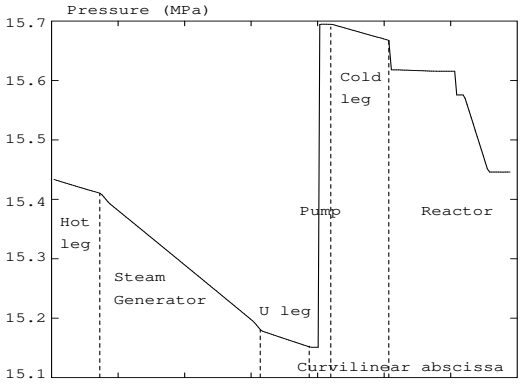

Figure 4: Pressure versus curvilinear abscissa

Copyright © 2000 by ASME

The figure 4 displays the pressure curve versus the curvilinear abscissa at 1.5 s in the loop 1 and the reactor along the main flow. The main flow goes through the reactor inlet, the lower part of the downcomer, the lower plenum, the core lower volume, the core, the lower part of the higher plenum and the reactor outlet.

The average computed pressure of the circuit is 15.43 MPa. It is very close to the theoretical average pressure of 15.5 MPa. The computed pressure losses fit in with the reactor nominal rating ones (Table 2).

	Nominal rating pressure losses (MPa)	Computed pressure losses (MPa)
Hot leg	0.026	0.025
Steam generator	0.232	0.232
U leg	0.027	0.027
Cold leg	0.027	0.028
Reactor inlet nozzle	0.049	0.049
Downcomer	0.002	0.002
Core support plate	0.040	0.040
Core	0.130	0.130
Reactor outlet nozzle	0.012	0.011

Table 2: Comparison of the theoretical and computed pressure losses in the circuit

The figure 5 presents the pressure map of the complete primary circuit at the time 1.5 s. The minimum and maximum pressures (respectively 15.17 and 15.7 MPa) are observed on both sides of the pumps. The cold legs are at 15.7 MPa. The pressure in the hot legs, the steam generators and the U legs decreases gradually from 15.4 to 15.2 MPa. The reactor pressure is situated around 15.5 - 15.6 MPa.

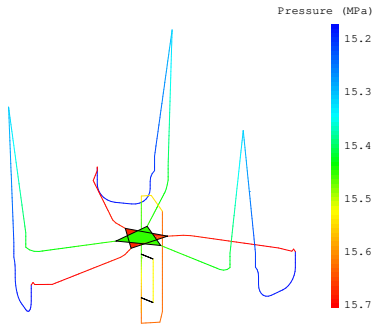

Figure 5: Pressure at t=1.5 s

The figure 6 shows the density map of the complete primary circuit at the time 1.5 s. The density is globally the same in the whole circuit: around the estimated 727 kg/m^3.

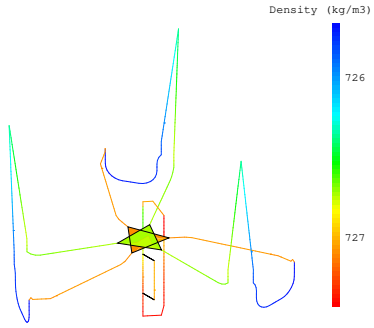

Figure 6: Density at t=1.5 s

The figure 7 exhibits the pump characteristics and its working point. The pump characteristics is defined as the pressure increment provided by the pump versus the volumic flow in the loop. The theoretical working point of the pump is (6.3 m^3/s ; 0.545 MPa = 76.4 m of water) if the average density is 727 kg/m^3.

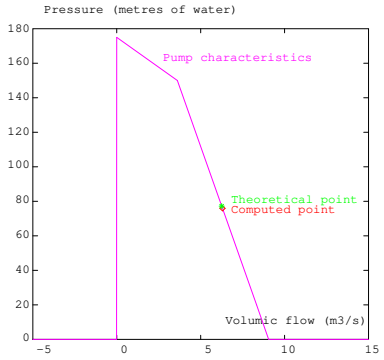

Figure 7: Pump working point

The computed working point is obtained from the figure 2 for the volumic flow, the figure 4 for the pump pressure increment and the figure 6 for the density. It is equal to (6.3 m^3/s ; 0.543 MPa = 76.13 m of water). The computed pump working point fit in with the theoretical one.

For all the scrutinized variables, we have seen that the computed results are very close to the theoretical results of the reactor nominal rating. Therefore, the model is correct and can be used for the LOCA computations.

Copyright © 2000 by ASME

3 Computation of the rupture

The computation of the LOCA is initialized with the same initial conditions as the nominal rating computation. Both calculations are not linked. Without information about the hydraulic characteristics of the circuit during a LOCA, we suppose that the reactor nominal rating pressure drops are available in accidental conditions.

A conventionnal double ended break is represented. The tear starts at the beginning of the LOCA computation and lasts 1 ms. It concerns the full section of the cold leg. The computation of the LOCA is carried out for 500 ms but, from the acoustic and dynamic points of view, the interesting results only concern the first 100 ms. The analysis of the results is focused on the pressures and the volumic flows.

3.1 Pressures in the complete circuit

The figures 8 display the pressure versus time at several points of loop 1 (broken loop), loop 2 and reactor. The graphics indicate at once the local pressure drop and the chronology of the acoustic wave propagation.

We observe a pressure drop with three phases:
- from 0 to 2 ms: a pressure drop at the break,
- from 2 to 100 ms: a general pressure loss in the whole circuit,
- after 100 ms: a slower diphasic pressure decrease in the primary circuit.

At the break (Fig. 8a and 8s), the pressure falls down from 15.5 MPa to 8.2 MPa for the first millisecond after the rupture. Then the pressure remains more or less stable around 8 MPa. As the saturation pressure is 8.6 MPa for a water temperature of 300°C, this result shows that, almost instantaneously, the pressure reaches the saturation pressure and the water becomes diphasic. After 2 ms, the pressure decrease is limited by the critical conditions at the break.

In the broken loop, two acoutic waves propagate from the break ends in opposite directions. They cause a progressive depressurization of the broken loop from the nominal rating conditions to about 8.2 MPa.

We note:
- "Wave 1": the wave coming from the reactor side,
- "Wave 2": the wave coming from the pump side,
- "Wave 3": the wave issued from the break on the reactor side and which crossed the reactor.

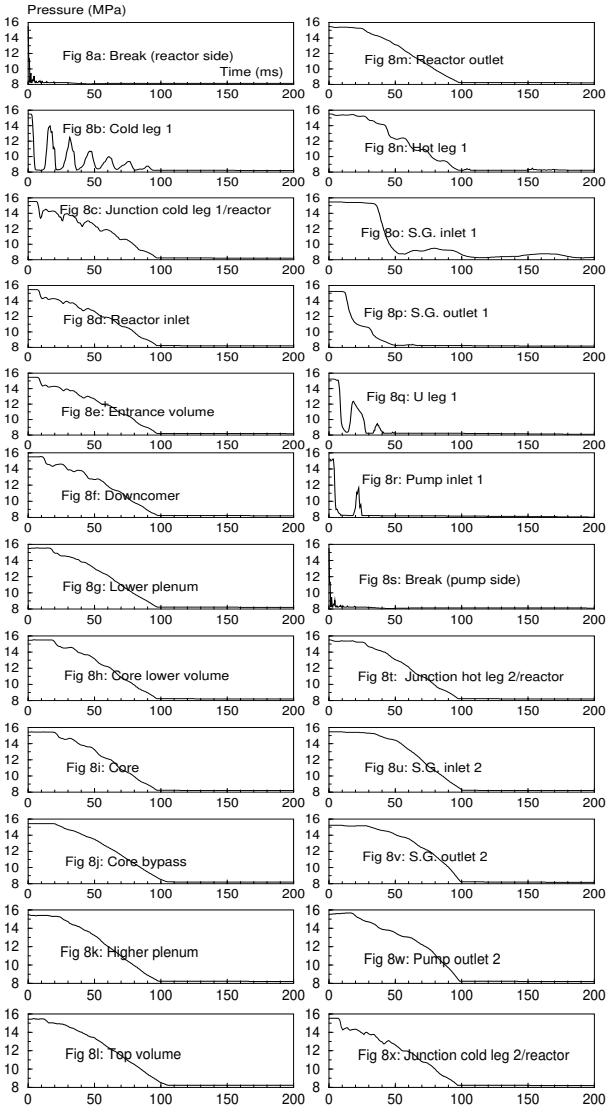

Figures 8: The pressure versus time

We observe pressure oscillations in the cold leg (Fig. 8b). They are due to successive partial reflections of the blowdown wave on the section change cold leg/reactor and on the pipe end because of the pressure boundary conditions imposed by the break. The oscillations damp out progressively because of the pressure losses by friction in the pipes.

Copyright © 2000 by ASME

The pressure at the junction between the cold leg and the reactor (Fig. 8c) is influenced by the connection between the three loops and the reactor. As in the non broken loops and the reactor, the saturation pressure is reached only after 100 ms. The decrease is jerked and we can observe the same oscillations than in the cold leg of the broken loop.

At the pump inlet (Fig. 8r), a pressure peak of 11.6 MPa occurs between 17 and 25 ms when the water becomes locally diphasic.

In the U leg (Fig. 8q), the pressure decreases until 8.2 MPa between 7 and 15 ms. In the same time, the flow increases in a monophasic regime because of the pressure difference between the steam generator and the break. ¿From 15 ms, the water becomes very slightly diphasic which stabilizes the volumic flow at critical flow. This slight vaporization causes a pressure increase until 12.4 MPa between 15 and 27 ms. The end of this pressure peak coincides with the beginning of a large vaporization phase. The second pressure peak between 32 and 42 ms is an attenuated version of the peak observed at the pump inlet.

At the steam generator outlet (Fig. 8p), the pressure fall slows down between 25 and 30 ms. Simultaneously, we observe a transient slowing down of the flow rate increase, imposed by the downstream flow conditions. The flat part of the curve is the superimposition of the blowdown wave and of the pressure peak observed in the U leg. The pressure only reaches the saturation pressure after 60 ms, just when the volumic flow gradient reverses.

At the steam generator inlet (Fig. 8o), we note a straight pressure fall because the water remains liquid.

In the hot leg (Fig. 8n), several blowdown waves superimpose. The first wave arrives at 28 ms after having crossed the reactor (wave 3). The second wave at 43 ms comes directly from the break on the pump side (wave 2).

In the non broken loops, the pressure falls down to 8.2 MPa in approximately 100 ms. The pressure conditions are identical at the junctions between the three loops and the reactor because the pipe model simplifies the connection geometry.

The acoustic wave 1 arrives in the cold legs in 8 ms (Fig. 8x). Then it propagates through the non broken loops. It arrives at the pump outlet in 18 ms (Fig. 8w) and at the steam generator outlet in 28 ms (Fig. 8v).

In the hot legs (Fig. 8t), we can see the passing of three different waves. The first one at 28 ms is the wave 3. The waves 1 and 2 arrive almost simultaneously at about 45 ms.

At the steam generator inlet (Fig. 8u), the slight pressure oscillations can be interpreted as: simultaneous arrival of waves 1 and 3 at 35 ms, arrival of wave 2 at 51 ms.

Crossing time (ms)	Wave 1	Wave 2	Wave 3
Break (reactor side)	1		
Cold leg 1	4		
Reactor inlet	7		
Entrance volume	8		
Downcomer	11		
Lower plenum	15		
Core lower volume	18		
Core and core bypass	21		
Higher plenum	23		
Top volume	13		
Reactor outlet	25	45	
Hot leg 1		43	28
Steam generator inlet 1		34	
Steam generator outlet 1		12	
U leg 1		7	
Pump inlet 1		5	
Break (pump side)		1	
Hot leg 2	45	43	28
Steam generator inlet 2	35	51	35
Steam generator outlet 2	28	58	48
Pump outlet 2	18		
Cold leg 2	8		

Table 3: Chronology of the crossing times of the blowdown waves

In the reactor, the pressure decreases from 15.5 MPa to 8.2 MPa in 100 ms. The reactor is crossed by the wave coming from the break on the reactor side. The oscillations, caused at the reactor inlet by the connection with the cold leg of the broken loop, lessen progressively when the wave runs along the reactor (Fig. 8d to 8i). The oscillations are deadened by the friction pressure losses in the reactor.

In the core bypass (Fig. 8j) and the top volume (Fig. 8l), the presence of high local pressure losses, imposed at the inlet and outlet of

Copyright © 2000 by ASME

these volumes to regulate the flow rate, leads to very smooth curves. The pressure in the higher plenum (Fig. 8k) and at the reactor outlet (Fig. 8m) is smoothened by the superimposition of the three different waves.

The table 3 summarizes the chronology of the propagation of the blowdown waves.

The figures 9 present the pressure of the complete circuit at different moments. Initially (Fig. 9a), the circuit is approximately at 15.5 MPa. After 10 ms (Fig. 9b), the cold leg, the pump and the U leg of the broken loop are depressurized. The pressure starts decreasing in the entrance volume and the non broken loop cold legs. The blowdown extends progressively to the whole broken loop in 50 ms (Fig. 9f).

The reactor becomes completely depressurized only after 80 ms (Fig. 9i). Meanwhile, we can observe non negligible pressure gaps between the different reactor zones. The reactor depressurization starts in the entrance volume (Fig. 9b) and propagates along the main circuit (downcomer, lower plenum, core lower volume, core and higher plenum). The last reactor zones to be depressurized (Fig. 9h) are the core bypass and the top volume: both volumes are cut off from the rest of the circuit because of the very weak flow rates going through them.

In the non broken loops, the depressurization starts in the cold legs at 10 ms (Fig. 9b) and in the hot legs at 30 ms (Fig. 9d). The last zones to be depressurized are the U legs and the steam generator outlet (Fig. 9i). The non broken loops are uniformly depressurized from 90 ms (Fig. 9j).

Between 100 ms (Fig. 9k) and 500 ms (Fig. 9l), the pressure remains constant in the complete circuit and equal to the saturation pressure.

3.2 Pressure differences in the reactor

The figures 10 display the pressure differences versus time between different points or zones of the reactor. The interesting zones are located near or around the core.

Horizontally, the pressure differences between the downcomer and the central part of the reactor come from the delay of the wave 1 crossing. Vertically, the gaps are due to the propagation time and the superimposition of several waves. The horizontal differences are higher than the vertical ones. All the gaps are observed during the first 100 ms, that means while the water remains liquid.

All the gaps are observed during the first 100 ms, that means while the water remains liquid. The highest gaps are always measured on the first peak of the curves, during the wave 1 crossing.

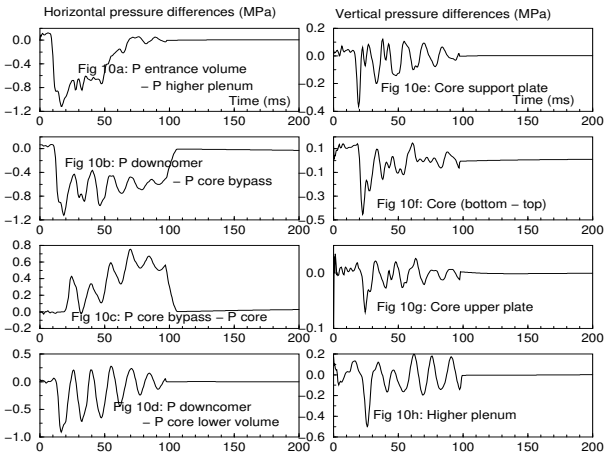

Figures 10: The pressure gaps versus time

The highest gaps, equal to 1.2 MPa, are located horizontally:

- between the entrance volume and the higher plenum (Fig. 10a), that means on the core barrel at the loop level,
- between the downcomer and the core bypass (Fig. 10b), on the core barrel halfway up the core.

The horizontal pressure difference on the core barrel at the core lower volume level, just below the core (Fig. 10d), is a little lower: 0.9 MPa. The pressure difference on the baffle assembly (Fig. 10c) reaches 0.8 MPa.

The horizontal pressure gaps can cause important strains and stresses on the core support and consequently interfer with the lateral core shape and the fuel assembly reactivity. All these pressure peaks take place between 15 and 20 ms after the rupture.

Copyright © 2000 by ASME

The vertical pressure differences are lower than the horizontal ones but not negligible. The gap on the core support plate (Fig. 10e), that means between the lower plenum and the core lower volume, reaches 0.4 MPa. The one between both core extremities (Fig. 10f) is equal to 0.55 MPa.

The gap read on the core upper plate (Fig. 10g) remains low: 0.07 MPa. As this plate is neither geometrically, nor hydraulically represented in our model, its influence is only globally taken into in the core pressure loss. So the result is imprecise.

The difference between the higher plenum extremities (Fig. 10h) reaches 0.6 MPa. This volume contains the guide tubes and the upper non radioactive part of the fuel assemblies. Their deformation immediately induces stresses in the rest of the assemblies.

The vertical pressure gaps are liable to cause buckling of the fuel assemblies. The gaps are observed between 20 and 26 ms, later than the horizontal gaps.

3.3 Flow rates in the complete circuit

The figures 11 display the volumic flow rate in the complete circuit at different moments. Before the break opening (Fig. 11a), the flow rate is 6.3 m^3/s in the loops and around 18 m^3/s in the reactor (except in the core bypass and the top volume where the flow rate is very low).

After the break opening (Fig. 11a), the flow accelerates in the pump and the U leg of the broken loop. In the cold leg of the broken loop, it starts reversing near the break whereas it remains slightly positive in the rest of the cold leg. The flow slightly slows down in the reactor main circuit and remains unchanged in the non broken loops.

At 20 ms (Fig. 11c) and 40 ms (Fig. 11d), the flow continues to accelerate in the U leg and the steam generator of the broken loop. In the cold leg, the flow is oriented towards the break now and starts to increase in this new direction. The flow rate diminishes in the main circuit of the reactor. It remains constant in the major part of the non broken loops.

From 60 ms to 100 ms (Fig. 11e to 11g), the flow rate towards the break increases in the whole broken loop. In the non broken loops, the flow rate decreases progressively in the hot legs and the steam generators while it increases in the cold legs, the pumps and the U legs. The water of the non broken loops is drained towards the break extremities: a water sharing line appears more or less in the steam generator tube bundle near the outlet.

In the reactor, the flow rate continues to reduce. The flow rate is higher at the reactor outlet (near the core) than at the reactor inlet (near the downcomer). As the reactor entrance is not very much supplied into water, the volumes near the entrance empty little by little. The last parts of the reactor main circuit to empty are the core and the higher plenum.

From 150 ms to 500 ms (Fig. 11h to 11l), the flow rate reduces progressively in the whole circuit. We note again the water sharing line in the non broken loops at the steam generator level.

The flow rate remains very low in the core bypass and the top volume during the whole computation because the cross sections at these volume extremities are very narrow. Therefore both volumes remain full of water at the end of the blowdown phase and the water they contain is available for the next phase of slow thermo-hydraulic emptying.

4 Conclusion

The hydrodynamic loads due to a LOCA were computed successfully with the CASTEM-PLEXUS code, by means of an hydraulic pipe-model of the complete primary circuit and the reactor. This paper mainly presents the results of the nominal rating computation and of the LOCA computation. The analysis concerns the pressures and the volumic flow rates. A similar computation with an improved break model and linked computations of the nominal rating and the LOCA is presented in (Robbe, 2000) for a 4-loop PWR.

References

Haar, L., Gallagher, J.S., Kell, G.S.: "NBS/NRC

 Copyright © 2000 by ASME

steam tables", National Standard Reference Data System, USA, (1984).
Hoffmann, A., Lepareux, M., Schwab, B., Bung, H.: "Plexus: A general computer program for fast dynamic analysis", Proc. Conf. Structural Analysis and Design on Nuclear Power Plant, Porto Alegre, Brazil, (1984).
Keim, E., et al., "Crack opening and leakage rates of real craks", Proc. ICONE-7407 (1999).
Lepareux[a], M., Schwab, B., Bung, H.: "Plexus: A general computer program for the fast dynamic analysis. The case of pipe-circuits", Proc. Smirt 8, Vol F1 2/1, (1985).
Lepareux[b], M., Schwab, B., Hoffmann, A., Jamet, P., Bung, H.: "Un programme général pour l'analyse dynamique rapide - Cas des tuyauteries", Proc. Colloque Tendances Actuelles en Calcul des Structures, Bastia, France (1985).
Libmann, J.: "Elements of nuclear safety", IPSN, Les editions de la physique, France (1996).
Ludmann, M., Sauvage, J.Y.: "LB LOCA analysis using the dterministic realistic methodology - Application to the 3 loop plant", Proc. ICONE-7413 (1998).
Moody, F.J.: "Maximum flow rate of a single component two-phase mixture", Journal of heat transfer, (February 1965).
Ohvo, J., Banati, J., Tuomainen, M., Kalli, H.: "Simulation of full-scale UPTF loop seal experiments with APROS, CATHARE and RELAP", Proc. ICONE-6090 (1998).
Papon, P., Leblond, J.: "Thermodynamique des états de la matière", Editeurs des Sciences et des Arts, Hermann, Paris, France, (1990).
Payan, F., Baratte, C., Tephany, F.: "Management of vibrations in piping systems", Proc. ICONE-6520 (1998).
Pretel, C., Reventos, F.: "Prediction of unusual occurrence of core dryout in SBLOCA scenarios of the ASCO NPP", Proc. ICONE-6529 (1998).
Riffard, C., Berton, J.L., Bignan, G., Ducret, P., Jeanneau, H., Gourmelon, Y.: "On-line primary flow monitoring in the PWR hot legs during in-service inspection using high temperature ultrasonic sensors", Proc ICONE-7002 (1999).
Robbe[a], M.F., Lepareux, M., Trollat, C.: "Hydrodynamic loads on a PWR primary circuit due to a LOCA. Pipe computations with the CASTEM-PLEXUS code", Proc. SMIRT 15, Vol J, (1999).
Robbe[b], M.F., Galon, P., Yuritzinn, T.: "Castem-Plexus : un logiciel de dynamique rapide pour évaluer l'intégrité des structures en cas d'accident", Revue Francaise de Mecanique, (1999) to appear.
Robbe, M.F., Potapov, S.: "A pipe-model to assess the hydrodynamic effects of a blowdown in a 4-loop PWR", Proc. ICONE-8186 (2000).
Royer, E., Toumi, I., "Cathare-Cronos-Flica coupling with Isas: a powerful tool for nuclear studies", Proc. ICONE-6472 (1998).
Sardain, P., Gautier, G.M., "Management of accidental transients in a PWR using a passive system", Proc. ICONE-6176 (1998).
Seligmann, D. et al., "Studies of vibrations of piping and nozzles", Proc. ICONE-6183 (1997).
Van Goethem, G., Keinhorst, G., Martin Bermejo, J., Zurita, A., "EC research on accident prevention and mitigation of severe accident consequences", Proc. ICONE-7374 (1999).
Weiss, P., Sawitzki, M., Winkler, F., "UPTF, a full-scale PWR loss-of-coolant accident experiment program", Atomkernenergie Kerntechnik Vol.49 n°1/2 (1986).

Copyright © 2000 by ASME

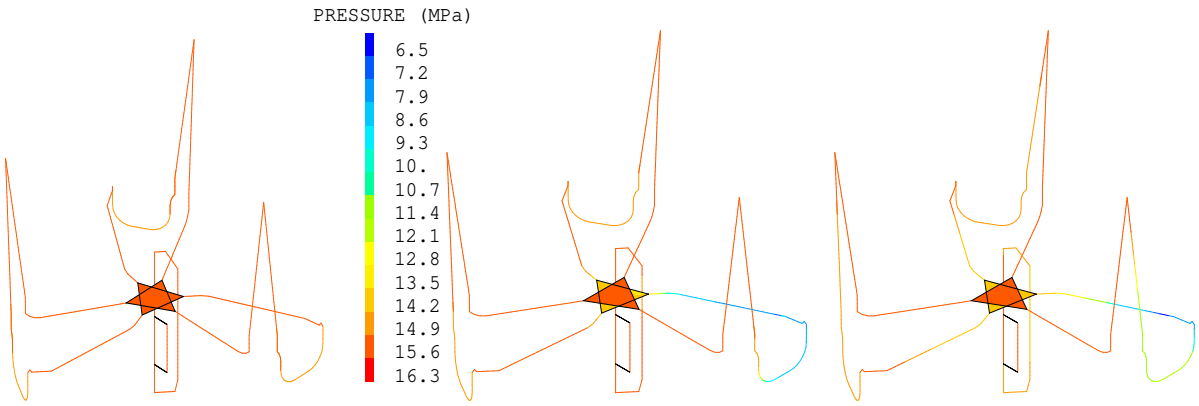

Fig 9a: Time 0 ms

Fig 9b: Time 10 ms

Fig 9c: Time 20 ms

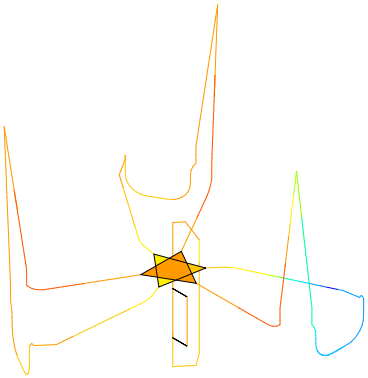

Fig 9d: Time 30 ms

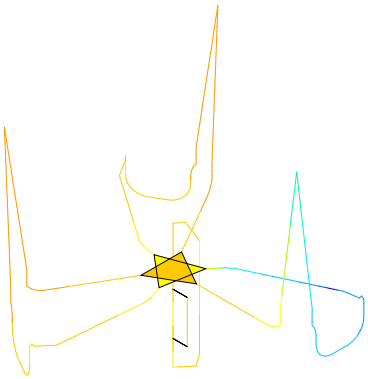

Fig 9e: Time 40 ms

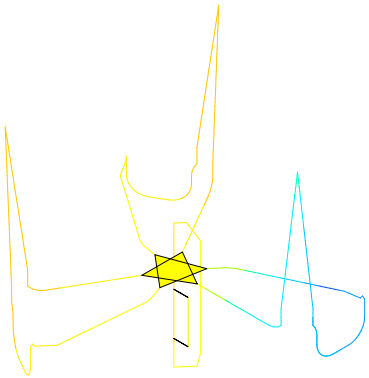

Fig 9f: Time 50 ms

Fig 9g: Time 60 ms

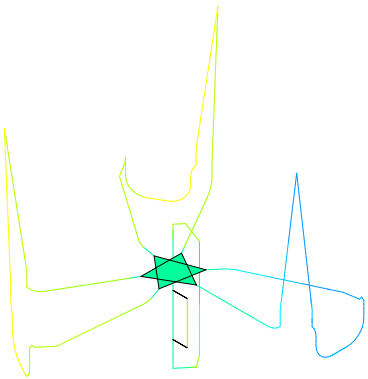

Fig 9h: Time 70 ms

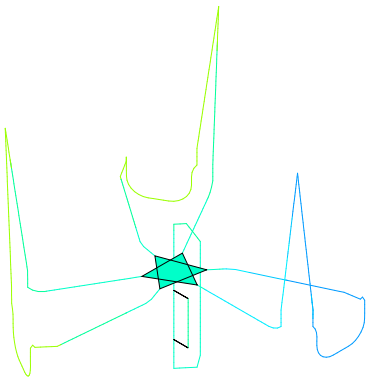

Fig 9i: Time 80 ms

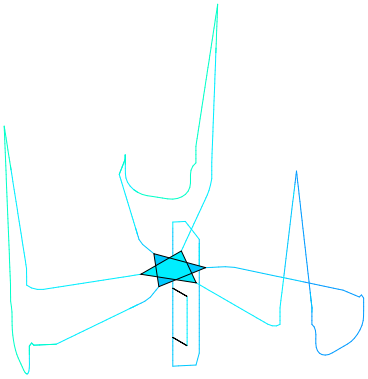

Fig 9j: Time 90 ms

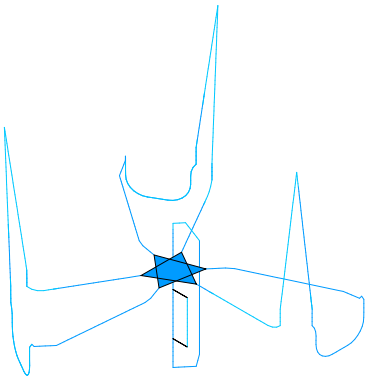

Fig 9k: Time 100 ms

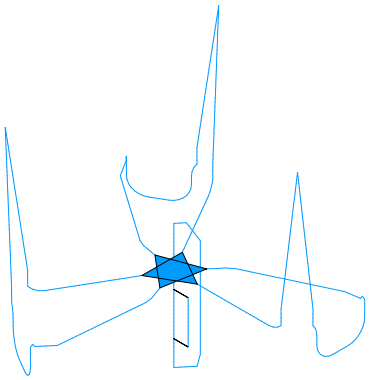

Fig 9l: Time 500 ms

Figures 9: Pressure in the circuit

Copyright © 2000 by ASME

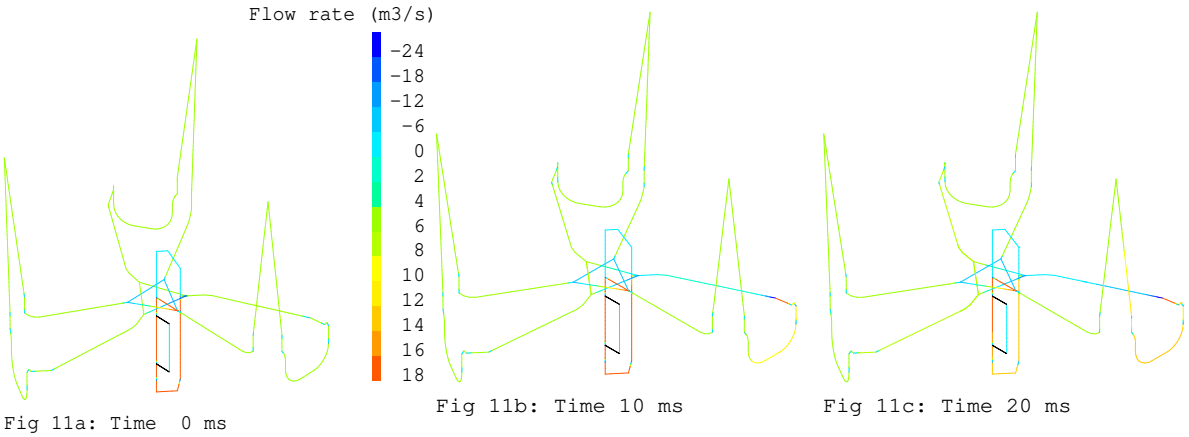

Fig 11a: Time 0 ms

Fig 11b: Time 10 ms

Fig 11c: Time 20 ms

Fig 11d: Time 40 ms

Fig 11e: Time 60 ms

Fig 11f: Time 80 ms

Fig 11g: Time 100 ms

Fig 11h: Time 150 ms

Fig 11i: Time 200 ms

Fig 11j: Time 300 ms

Fig 11k: Time 400 ms

Fig 11l: Time 500 ms

Figures 11: The volumic flow rate in the circuit

Copyright © 2000 by ASME